J Membrane Biol (2009) 228:111–124
DOI 10.1007/s00232-009-9164-6

Sequence- or Position-Specific Mutations in the Carboxyl-Terminal FL Motif of the Kidney Sodium Bicarbonate Cotransporter (NBC1) Disrupt Its Basolateral Targeting and α-Helical Structure

Hong C. Li · Joel H. Collier · Ali Shawki · Jai S. Rudra · Emily Y. Li · Bryan Mackenzie · Manoocher Soleimani

Received: 5 January 2009 / Accepted: 18 February 2009 / Published online: 18 March 2009

Abstract The sodium-bicarbonate cotransporter NBC1 is targeted exclusively at the basolateral membrane. Mutagenesis of a dihydrophobic FL motif (residues 1013–1014) in the C-terminal domain disrupts the targeting of NBC1. In the present study, we determined the precise constraints of the FL motif required for basolateral targeting of NBC1 by expressing epitope-tagged wild-type and mutant NBC1 in MDCK cells and RNA-injected *Xenopus* oocytes and examining their subcellular localization. We assayed the functional activity of the mutants by measuring bicarbonate-induced currents in oocytes. Wild-type NBC1 (containing PFLS) was expressed exclusively on the basolateral membrane in MDCK cells. Reversal of the FL motif (PLFS) had no effect on basolateral targeting or activity. Shifting the FL motif one residue upstream (FLPS) resulted in mistargeting of the apical membrane but the FLPS mutant retained its functional activity in oocytes. Shifting the FL motif one residue downstream resulted in a mutant (PSFL) that did not efficiently translocate to the plasma membrane and was instead colocalized with the ER marker, protein disulfide isomerase (PDI). Analysis of circular dichroism (CD) revealed that a short peptide, 20 amino acid residues, of wild-type NBC1 contained a significant α-helical structure, whereas peptides in which the FL motif was reversed or C-terminally shifted were disordered. We therefore propose that the specific orientation and the precise location of the FL motif in the primary sequence of NBC1 are strict requirements for the α-helical structure of the C-terminal cytoplasmic domain and for targeting of NBC1 to the basolateral membrane.

Keywords Acid-base transporters · Intestinal and renal transport · Epithelial transport · Intracellular pH regulation

H. C. Li · E. Y. Li · M. Soleimani
Center on Genetics of Transport, University of Cincinnati, Cincinnati, OH, USA

H. C. Li (✉) · E. Y. Li · M. Soleimani (✉)
Department of Internal Medicine, University of Cincinnati, 231 Albert Sabin Way, M. L. 0585, Cincinnati, OH 45267-0585, USA
e-mail: Hong.Li@uc.edu

J. H. Collier · J. S. Rudra
Department of Surgery, University of Chicago, Chicago, IL 60637, USA

A. Shawki · B. Mackenzie
Department of Molecular and Cellular Physiology, University of Cincinnati, Cincinnati, OH 45267, USA

M. Soleimani
Research Services, Veterans Administration Medical Center, Cincinnati, OH 45220, USA
e-mail: Manoocher.Soleimani@uc.edu

Polarized epithelial cells fulfill their physiological functions by specific sorting, trafficking, and targeting of apically and basolaterally localized transmembrane proteins (Tepass et al. 2001). Several molecular mechanisms have been described for the polar distribution of membrane proteins, including N-linked glycosylation (Scheiffele et al. 1995; Gut et al. 1998), association with glycosphingolipids (GPIs) (Brown and Rose 1992), and binding of lipid rafts (Simons and Ikonen 1997; Ikonen 2001), which are shown to be among the essential pathways that can direct the targeting of a membrane protein at the apical membrane

(Kundu et al. 1996; Lin et al. 1998; Barman et al. 2001; Muth and Caplan 2003).

In contrast, few models exist for the basolateral targeting of transmembrane proteins, and these are based on specific cytoplasmic motifs in N- or C-terminal cytoplasmic domains. Tyrosine-to-alanine substitutions in the tyrosine-based motif NPXY/YXXφ (φ being defined as a bulky or hydrophobic residue) of the low-density lipoprotein receptor (LDL-R) (Matter 1992), the vesicular stomatitis virus glycoprotein (VSVG) (Thomas et al. 1993), the polymeric immunoglobulin A receptor (pIgA-R), the transferrin receptor (TfR), or the anion exchanger 1 (AE1) (Matter et al. 1992, 1994; Thomas et al. 1993; Matter and Mellman 1994; Devonald et al. 2003; Mackenzie et al. 2007) disrupt the exclusive basolateral targeting of these proteins. Di-leucine motifs are thought to be critical for exclusive targeting of several proteins at the basolateral membrane in polarized epithelial cells, including the IgG Fc receptor FcRII-B2 (FcR) (Matter and Mellman 1994; Hunziker and Fumey 1994), E-cadherin, nucleotide pyrophosphatase/phosphodiesterase1 (NPPase1), sulfate anion transporter sat-1, and ClC2 chloride channel (Miranda et al. 2001; Bello et al. 2001; Regeer and Markovich 2004; Pena-Munzenmayer et al. 2005). In addition, leucine-leading or valine-leading dihydrophobic motifs are thought to participate in basolateral targeting of transmembrane proteins, and these include the Leu-Val(LV) motif in CD44 (resident plasma membrane adhesion protein) (Sheikh and Isacke 1996), the Leu-Ile(LI) motif in PMCA (1b, 2b) (plasma membrane Ca^{2+}-ATPase) (Grati et al. 2006), the VV motif (valine^{333}/valine^{334}) in the carboxyl-terminal cytoplasmic portion of the Kir4.1 channel in renal distal tubules (Tanemoto et al. 2005), and the VW motif in the N-terminal cytoplasmic domain of NaDC3 (sodium-dependent dicarboxylate transporter) (Bai et al. 2006). Further characterization of these dihydrophobic motifs is needed.

Recently, the FL dihydrophobic motif was shown to play an important role in the basolateral targeting of the sodium bicarbonate cotransporter (NBC1, SLC4A4) in MDCK cells (Li et al. 2004, 2007). In the kidney proximal tubule, basolateral Na^+:HCO_3^- cotransporter NBC1 functions in tandem with apical Na^+/H^+ exchanger 3 (NHE3) in the kidney proximal tubule and is essential for reabsorption of the majority of filtered bicarbonate (Romero et al. 1997, 2004, 2005; Burnham et al. 1997; Soleimani and Burnham 2001; Soleimani 2002, 2003; Abuladze et al. 2005; Pushkin and Kurtz 2006; Boron 2006). Certain mutations were reported to cause mistargeting of NBC1 to the apical membrane or the cytoplasm in MDCK polarized cells (Li et al. 2005; Toye et al. 2006), resulting in bicarbonate wasting and proximal renal tubular acidosis in human probands (Igarashi et al. 1999, 2001; Usui et al. 2001; Alper 2002; Dinour et al. 2004; Horita et al. 2005).

In order to better understand the targeting signals of the dihydrophobic FL motif in NBC1, the FL-containing motif was subjected to reverse motif sequence or position alteration in order to ascertain the importance of the specific orientation and flexibility of its primary sequence. The mutants were epitope tagged, transiently transfected in polarized MDCK cells, and visualized by confocal microscopy. In parallel studies, NBC1 wild-type and mutants were expressed in *Xenopus laevis* oocytes and their activities examined using the voltage clamp. The secondary structures of the wild-type dihydrophobic FL motif and mutants of interest were further examined by circular dichroism technique with synthesized short peptides.

Materials and Methods

Construction of Tagged Wild-Type and Mutant NBC1

Full-length NBC1 was generated by PCR, using human full-length kidney NBC1 cDNA (3257 bp, coding for 1035 amino acid residues) as a template (GenBank no. AF007216). Amplified wild-type NBC1 DNA was fused translationally in-frame to GFP by cloning it into the pcDNA3.1/NT-GFP-TOPO vector (Invitrogen, Carlsbad, CA). Site-directed mutagenesis was performed using the QuikChange Site-Directed Mutagenesis Kit (Stratagene, La Jolla, CA). Schemes 1 and 2 depict the locations of various mutations and primers used for these studies. The GFP-kNBC1 mutant with a reversed FL (P**LF**S) motif was generated using its sense and antisense primers and a previously generated GFP-kNBC1 mutant FF cDNA as a template (Li et al. 2007). In order to generate the GFP-kNBC1 mutant (**FL**PS) with the FL motif shifted upstream, the GFP-kNBC1 mutant intermediate 1{L(1012)L1013) P(1014)S(1015)} was first generated using its sense and antisense primers and GFP-kNBC1 mutant LL cDNA as a template, shown in Scheme 1. Thereafter, the GFP-kNBC1 mutant (**FL**PS) with the FL motif shifted upstream was generated using its sense and antisense primers and GFP-kNBC1 mutant intermediate 1 cDNA as a template. In order to generate the GFP-kNBC1 mutant (PS**FL**) with the FL motif shifted downstream, the GFP-kNBC1 mutant intermediate 2{P(1012)F1013)F(1014)L(1015)} was generated using its sense and antisense primers and another previously generated GFP-kNBC1 mutant FF cDNA as a template (Li et al. 2007). Then the GFP-kNBC1 mutant (PS**FL**) with the FL motif shifted downstream was generated using its sense and antisense primers and GFP-kNBC1 mutant intermediate 2 cDNA as a template, as shown in Scheme 1. Cycling parameters for the QuikChange site-directed mutagenesis experiments were as follows:

Scheme 1 Amino acid sequence and location of GFP-kNBC1 mutants

GFP-kNBC1 P**LF**S

GFP-kNBC1 wild-type:	**QQP(1012)F(1013) L(1014) S(1015)**
GFP-kNBC1 mutant FF(Li, et al., 2007):	**QQP(1012)F(1013) F(1014) S(1015)**
GFP-kNBC1 mutant 1(FL motif reversed):	**QQP(1012)L(1013)F(1014)S(1015)**

GFP-kNBC1 **FL**PS

GFP-kNBC1 wild-type:	**QQP(1012)F(1013) L(1014) S(1015)**
GFP-kNBC1 mutant LL(Li, et al., 2007):	**QQP(1012)L(1013) L(1014)S(1015)**
GFP-kNBC1 mutant intermediate 1(LLPS,):	**QQL(1012)L(1013)P(1014)S(1015)**
GFP-kNBC1 mutant 2(FL upstream shifted):	**QQF(1012)L(1013)P(1014)S(1015)**

GFP-kNBC1 PS**FL**

GFP-kNBC1 wild-type:	**QQP(1012)F(1013) L(1014) S(1015)**
GFP-kNBC1 mutant FF(Li, et al., 2007):	**QQP(1012)F(1013) F(1014) S(1015)**
GFP-kNBC1 mutant intermediate 2(PFFL):	**QQP(1012)F(1013) F(1014) L(1015)**
GFP-kNBC1 mutant 3(FL downstream shifted):	**QQP(1012)S(1013) F(1014) L(1015)**

segment 1—95°C, 30 s, 1 cycle; and segment 2—95°C, 30 s, 55°C, 1 min, 68°C, 10 min, 16 cycles. The sequences of all mutants were confirmed by sequencing at either the DNA Core Facility, Cornell University, or DNA Analysis, LLC, Cincinnati, OH.

Transient Expression of Epitope-Tagged Wild-Type NBC1 and NBC1 Mutants in MDCK Cells

The pcDNA3.1/NT-GFP-NBC1-TOPO or pcDNA3.1/GFP-NBC1 constructs were transformed into TOP 10 competent cells and single colonies were picked for growing in 1 ml TB bacterial culture medium for 8 h and then transferred to 50 ml TB culture medium for growing overnight. The Qiagen EndoFree Plasmid Maxi Kit (Qiagen, Valencia, CA) was used to prepare and purify endotoxin-free plasmids. MDCK cells were maintained in culture medium (DMEM) supplemented with 25 mM $NaHCO_3$, 10% fetal calf serum, penicillin (50 U/ml), and streptomycin (50 μg/ml) and incubated at 37°C in 5% CO_2/95% air. MDCK cells were transiently transfected with tagged or tag-free NBC1 full-length constructs and mutants and studied 48–72 h later according to established methods (Li et al. 2004, 2005, 2007). Briefly, cells were seeded on coverslips and transfected at 80% confluence using 1 μg of DNA and 4 μl of Lipofectamine 2000 (Invitrogen). Transfection efficiency was monitored using PCMV-SPORT β-gal plasmid as control. Changes in cell color in response to X-gal addition were used as marker for β-gal expression. All cells were colabeled with phalloidin-tetramethylrhodamine or PNA-lectin Alexa Fluor 568 conjugate, as marker of membrane labeling. Transient expression experiments were conducted three separate times for each construct.

Expression of Wild-Type and Mutant NBC1 in Oocytes

We performed laparotomy and ovariectomy on adult female *Xenopus laevis* frogs under 2-aminoethylbenzoate methanesulfonate anesthesia (0.1% in 1:1 water/ice, by immersion) following a protocol approved by the University of Cincinnati Institutional Animal Care and Use Committee. Ovarian tissue was isolated and treated with collagenase A (Roche Diagnostics), and defolliculate stage V–VI oocytes were isolated as described (Mackenzie 1999). We generated

Scheme 2 Primer sequences for NBC1 mutants

GFP-kNBC1 wild type,	Q Q P(1012) F(1013) L(1014) S(1015)
GFP-kNBC1 mutant P**LF**S{FL motif reversed):	Q Q P(1012) L(1013) F(1014) S(1015)
Sense:	**5' CATGGAACAGCAACCTTTGTTCAGCGATAGCAAAC CTTCTG 3', 41mer .**
Antisense:	**5' CAGAAGGTTTGCTATCGCTGAACAAAGGT TGCTGTTCCATG 3', 41mer**
GFP-kNBC1 mutant **FL**PS{FL motif shifted upstream) : Q Q F(1012) L(1013) P(1014) S(1015)}	
Sense:	**5'GGACATCATGGAACAGCAATTTTTGCCAAGCGATAGCAAACC3', 42mer**
Antisense:	**5' GGTTTGCTATCGCTTGGCAAAAATTGCTGTTCCATGATGTCC3', 42mer**
GFP-kNBC1 mutant PS**FL** {FL motif shifted downstream): Q Q P(1012) S(1013) F(1014) L(1015)	
Sense:	**5'ATCATGGAACAGCAACCTTCCTTCCTCGATAGCA AACCT 3', 39mer**
Antisense:	**5'AGGTTTGCTATCGAGGAAGGAAGGTTGCTG TTCCA TGAT3', 39mer**
GFP-kNBC1 mutant intermediate 1	
Sense:	**5' GACATCATGGAACAGCAACTTTTGCCAAGCGATAGCAAACC3', 41 mer**
Antisense:	**5'GGTTTGCTATCGCTTGGCAAAAGTTGCTGTTCCATGATGTC 3', 41 mer**
GFP-kNBC1 mutant intermediate 2	
Sense:	**5' CATGGAACAGCAACCTTTCTTCCTCGATAGCAAACCTTCTG 3', 41mer**
Antisense:	**5'CAGAAGGTTTGCTATCGAGGAAGAAAGGTTGCTGTTCCATG 3', 41mer**

capped tag-free (no GFP) or tagged (GFP-NBC1 full-length, GFP-NBC1 point mutations, and GFP only) NBC1 cRNAs as described (Li et al. 2004, 2005, 2007; Xu et al. 2003) using the mMESSAGE mMACHINE T7 Kit (Ambion, Inc., Austin, TX) according to the manufacturer's instructions. We injected oocytes with ≈50 ng cRNA and incubated the oocytes at 17°C in modified Barths' medium (Mackenzie 1999) for 3–4 days prior to Western blotting, immunocytochemistry, or voltage-clamp experiments.

Confocal Microscopy and Immunofluorescence Labeling of Epitope-Tagged Wild-Type and Mutant NBC1 in MDCK Cells and Xenopus Oocytes

MDCK cells were washed with PBS and fixed in 4% formaldehyde/PBS solution as described (Li et al. 2004, 2005, 2007). For colabeling studies, MDCK cells were costained with PNA-lectin Alexa Fluor 568 conjugate (Molecular Probes, Eugene, OR) for 30 min. In separate studies, cells were permeabilized with 0.1% Triton X-100 in PBS, washed with PBS, and costained with phalloidin-tetramethylrhodamine (Sigma, St. Louis, MO) for 30 min. Afterward, cells were washed with PBS and mounted on glass slides in Vectashield mounting medium for fluorescence (Vector Laboratories, Inc., Burlington, CA). Images were acquired on a Zeiss LSM510 confocal microscope. Both Z-line (y-z or x-z projection) and Z-stack (x-y projection) images were obtained using the LSM 5 Image software (Li et al. 2004, 2005, 2007). Generally, 0.4- to 1.0-μm fixed-interval cuts were obtained, and 20–30 images were generated as a gallery. Z-stack images were chosen from the first three to six basal sections, and images (x-y projections) and corresponding z-lines (x-z or y-z projections) were obtained.

Mouse anti ZO-1 antibody purchased from Zymed (catalog no. 33-9100; San Francisco, CA) and mouse anti-PDI (protein disulfide isomerase) purchased from Stressgen Bioreagents (catalog no. SPA-891; Victoria, BC, Canada) were diluted 200 times and used for immunofluorescence labeling.

Donkey anti-mouse or rabbit Alexa-Fluor 568-conjugated secondary antibodies were used to stain MDCK cells or *X. laevis* oocyte sections according to established methods and as reported from our laboratory (Xu et al. 2003; Li et al. 2005). Three slides from three independent

transient expression experiments were stained. *X. laevis* oocytes expressing GFP alone, GFP-kNBC1, or GFP-kNBC1 mutant PS**FL** were embedded in OCT compound and frozen on dry ice. Samples were cryostat-sectioned at 7-μm thickness and stained with rabbit anti-GFP serum (1:500) and Alexa-Fluor 568-conjugated secondary antibody (1:200) (rabbit anti-GFP serum purchased from Invitrogen; catalog no. A6455).

Each plasmid construct was also expressed in filter-grown polarized MDCK cells. A 24-well cluster with 0.4-μm-pore size filters (Costar) was used to grow MDCK cells and transiently transfect with endotoxin-free plasmid DNAs of GFP, GFP-kNBC1 wild-type, and mutants. Polarized MDCK cells were transiently transfected with epitope-tagged kNBC1 wild-type and mutant PS**FL** endotoxin-free plasmids and costained with a mouse anti-PDI antibody (1:500) and Alexa-Fluor 568-conjugated secondary antibody (1:200).

Western Blot Analysis

Oocytes were homogenized in lysis buffer in the presence or absence of 1% Triton X-100. Each fraction was centrifuged at 14,000 *g* and the resultant supernatant was saved. The lysis buffer without detergent consists of 30 mM Tris, 20 mM MES, 100 mM NaCl, final pH 7.0. The lysis buffer contained a mixture of protease inhibitors (Complete Mini, EDTA-free Protease inhibitor cocktail tablets; Ref no. 11-836-170-001; Roche Diagnostics, Indianapolis, IN). Western blot analysis of detergent and nondetergent fractions were performed according to established methods (Zou et al. 2004; Li et al. 2005) using GFP-specific polyclonal antibody (Invitrogen) at a 1:500 dilution. Donkey anti-rabbit IgG-horseradish peroxidase (HRP) was used as the secondary antibody (Pierce, Rockford, IL). Goat *β*-actin polyclonal antibody (1:1000) was used (Santa Cruz Biotechnology, Santa Cruz, CA) as a control for loading, with rabbit anti-goat IgG-HRP (1:1000) as the secondary antibody (The Jackson Laboratory, Bar Harbor, ME). The antigen-antibody complex was detected by the chemiluminescence method using the SuperSignal West Pico Chemiluminescent Substrate Kit (Pierce). Experiments were repeated at least three times and GFP protein expression was normalized by *β*-actin labeling on the same blot.

Functional Assay of NBC1 Activity in Oocytes

We used a two-microelectrode voltage clamp (Dagan CA-1B amplifier) as described (Mackenzie et al. 2007) to measure currents in control oocytes and oocytes expressing epitope-tagged wild-type or mutant kNBC1. Microelectrodes with a resistance of 0.5–5 MΩ were filled with 3 M KCl. Oocytes were clamped at $V_h = -50$ mV, and step changes in membrane potential (V_m) were applied from −160 to +40 mV (in 20-mV increments), each for a duration of 100 ms, before and after the addition of bicarbonate. Current was low-pass-filtered at 500 Hz and digitized at 5 kHz. Steady-state data were obtained by averaging the points over the final 16.7 ms at each V_m step. Oocytes were superfused at 23°C with ND96 medium of the composition (in mM) 96 NaCl, 2 KCl, 1 $MgCl_2$, 1.8 $CaCl_2$, and 15 Hepes (pH 7.5 with Tris base) and, subsequently, with ND96 in which 33 mM NaCl was replaced with 33 mM $NaHCO_3$ equilibrated with 5.6% CO_2/94.4% N_2.

Peptide Synthesis

A 20-amino-acid peptide from wild-type NBC1 with the sequence IKIPMDIMEQQP**FL**SDSKPS encompassing residues I1001–S1020 [highlighted as P**FL**S], kNBC1 mutant P**LF**S with the sequence IKIPMDIMEQQP **LF**SDSKPS, or kNBC1 mutant PS**FL** with the sequence IKIPMDIMEQQP**SFL**DSKPS were designed and synthesized by solid-state phase synthesis at GenScript Corp., Piscataway, NJ. Peptides were synthesized from C-terminus to N-terminus by Fmoc {*N*-(9-fluorenyl)methooxycarbonyl}chemistry on an Applied Biosystem 433A peptide synthesizer. The short peptides were started from Fmoc-Ser{tBu(t-butyl)}-Wang resin (4-benzyloxybenzyl alcohol resin) and then coupled with the next Fmoc protected amino acid in one synthesis cycle with the aid of HOBt(*N*-hydroxybenzotriazole)/DIC(*N,N*-diisopropylcarbodiimide). After full sequences were completed, they were cleaved from resin with a TFA (trifluoroacetic acid) cocktail solution and crystallized in ether. Crude samples were purified by RP-HPLC C18 (reversed preparative high-performance liquid chromatography) columns under a gradient of ACN (acrylonitrile) + 0.1% TFA and H_2O + 0.1 TFA washing buffer and verified by mass spectrometry analysis. All resultant peptides are >95% pure.

Circular Dichroism Analysis

An AVIV 215 circular dichroism (CD) spectropolarimeter (Aviv Biomedical, Lakewood, NJ) was used with 0.1-cm-path-length quartz cells. Stock solutions of 1 mM peptide at pH 7.2 were prepared in phosphate buffer (10 mM sodium phosphate, 10 mM potassium fluoride). Chloride-containing buffers were avoided to minimize CD signal diminishment. Samples were diluted to a working concentration of 60 μM in CD buffer with or without 50% TFE, and triplicate scans were averaged at 25°C. Under these conditions, adequate signal strength was observed, and PMT dynode voltage values were <500 V for wavelengths >190 nm. All CD spectra are reported as mean residue ellipticity (deg cm^2 $dmol^{-1}$) (Greenfield 2006).

Statistics

Data are presented as mean ± SE. We used repeated-measures ANOVA followed by Holm-Šidák multiple comparisons to test between-group inferences, with a critical significance level (α) of 0.05.

Materials

A high-fidelity PCR Amplification Kit, GFP Fusion TOPO TA Expression Kit, and Lipofectamine 2000 were purchased from Invitrogen. EndoFree Plasmid Maxi Kit was purchased from Qiagen. DMEM was purchased from Life Technologies. Other chemicals (except where indicated) were purchased from Sigma Co. (St. Louis, MO).

Results

Full-Length NBC1 is Targeted Exclusively at the Basolateral Membrane in MDCK Epithelial Cells

In the first series of experiments, we examined the expression of GFP vector without the NBC1 insert in MDCK cells. Figure 1a (x-y projection) shows that the GFP vector alone (no NBC1 insert) results in the accumulation of GFP in the cytoplasm, when merged images with the cell junction marker ZO-1 is obtained. However, transfection with GFP-NBC1 full-length cDNA shows an exclusive localization on the cell membrane as visualized by x-y projections, front view (Fig. 1b, top and middle; colabeled with ZO-1 staining). Z-line image (Fig. 1b, bottom; x-z projection) analysis indicates that NBC1 is exclusively detected on the basolateral membrane. These results were also confirmed in polarized MDCK cells costained with phalloidin-tetramethylrhodamine (Fig. 1c). The results in Fig. 1b, c are consistent with published reports on the basolateral membrane localization of NBC1 in epithelial cells (Roussa et al. 1999; Schmitt et al. 1999; Thevenod et al. 1999; Bok et al. 2001; Yamada et al. 2003; Li et al. 2004, 2005, 2007; Toye et al. 2006).

Reversal of the FL Motif Does Not Affect the Basolateral Targeting of NBC1

Transfection with the GFP-NBC1 mutant P**LF**S shows exclusive localization on the cell membrane, as visualized by x-y projections, front view (Fig. 2a, top and middle; colabeled with ZO-1 staining). Z-line image (Fig. 2a, bottom; x-z projection) analysis indicates that NBC1 mutant P**LF**S is exclusively detected on the basolateral membrane, which is also confirmed in polarized MDCK cells costained with phalloidin-tetramethylrhodamine (Fig. 2b).

Shifting of the FL Motif Upstream Causes Mistargeting of NBC1 at the Apical Membrane

Transfection with the GFP-NBC1 mutant **FL**PS, encoding a dihydrophobic FL motif that is shifted upstream by one residue, shows cell membrane localization as visualized by Z-stack images (Fig. 3a, bottom and middle; x-y projections). The x-z projections, side view, show the apical membrane localization of the mutant **FL**PS in transfected cells (Fig. 3a, top; colabeled with ZO-1 staining). The apical membrane localization of mutant **FL**PS was also confirmed in polarized MDCK cells costained with phalloidin-tetramethylrhodamine and PNA-lectin (Fig. 3b).

Shifting of the NBC1 FL Motif Downstream Causes Mistargeting of NBC1 at the Cytoplasm

Transfection with the GFP-NBC1 mutant P**SFL** encoding a dihydrophobic FL motif that is shifted downstream by one residue, shows a predominantly cytoplasmic localization, as visualized by x-y projections, front view (Fig. 4a, bottom and middle; colabeled with ZO-1 staining). Z-line image (Fig. 4a, top; x-z projection) analysis indicates that the mutant P**SFL** also shows some apical membrane staining. The cytoplasmic and residual apical localization of the P**SFL**-containing mutant was also confirmed in polarized MDCK cells costained with phalloidin-tetramethylrhodamine and PNA-lectin (Fig. 4b).

Functional Activities of NBC1 Mutants Expressed in Oocytes

Bicarbonate-induced currents in oocytes expressing kNBC1 mutants P**LF**S and **FL**PS did not differ from those in wild-type kNBC1 (Fig. 5). In contrast, bicarbonate-induced currents mediated by the kNBC1 mutant P**SFL** were significantly reduced relative to wild-type NBC1; however, we observed no qualitative difference in current-voltage relationships between P**SFL** and wild-type kNBC1, suggesting that the lower activity for P**SFL** resulted from its reduced expression at the plasma membrane and did not result from altered properties of Na^+/HCO_3^- cotransport.

The FL Motif Which is Shifted Downstream Shows Reduced Surface Membrane Expression in Oocytes and Colocalizes with ER Marker PDI in Polarized MDCK Cells

To determine whether the expressed proteins are in membrane-containing detergent fractions, cRNA-injected

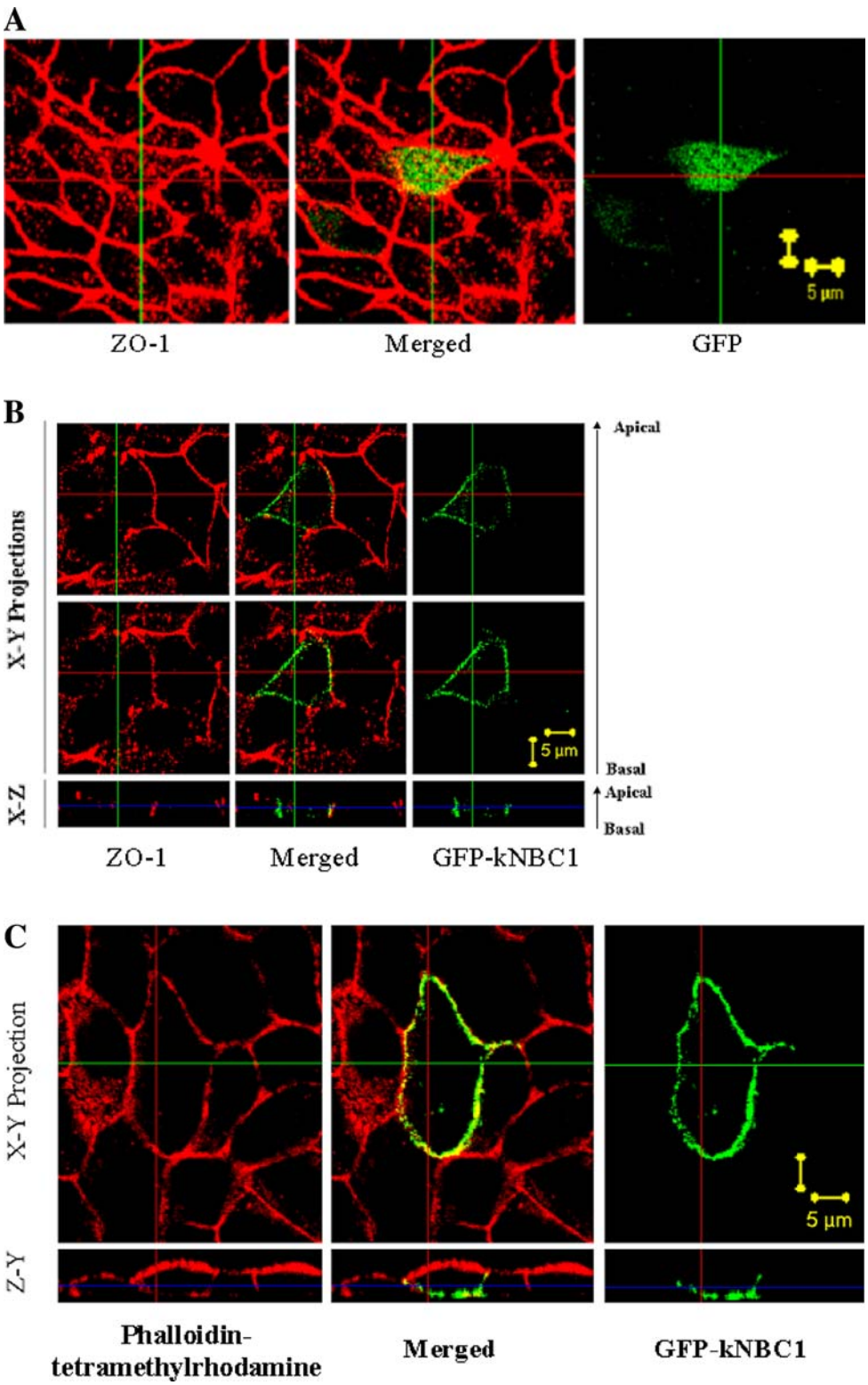

Fig. 1 Transfection of MDCK cells with GFP vector only (no NBC1 insert) or tagged wild-type NBC1. **a** Expression of GFP vector only (no NBC1 insert) costained with ZO-1. Z-stack analysis (x-y projection, front view). The result indicates that transfection with GFP vector alone, with no NBC1 insert, results in the accumulation of GFP in the cytoplasm and does not reach the plasma membrane. **b** Expression of epitope-tagged wild-type NBC1 (1010 QQP**FL**S 1015) costained with ZO-1. Z-stack (x-y projections, front view) image analysis (top and middle). As demonstrated, full-length NBC1 is targeted at the plasma membrane. Z-line (x-z projection, side view) image analysis (bottom). As demonstrated, full-length NBC1 is exclusively targeted at the basolateral membrane. Green, GFP or GFP-NBC1; red, ZO-1 staining with Alexa-Fluor 568. **c** Expression of epitope-tagged wild-type NBC1 (1010 QQP**FL**S 1015) costained with phalloidin-tetramethylrhodamine. Z-stack (x-y projections, front view) image analysis (top). As demonstrated, full-length NBC1 is targeted at the plasma membrane. Z-line (z-y projection, side view) image analysis (bottom). As shown, full-length NBC1 is exclusively targeted at the basolateral membrane. Green, GFP-NBC1; red, phalloidin-tetramethylrhodamine staining

oocytes were homogenized in lysis buffers with or without 1% Triton X-100 and fractioned mixtures were loaded onto SDS-PAGE gels for Western blot analysis. Rabbit anti-GFP antibodies were used to detect the GFP signal. In extracts using detergent-containing buffer, we detected abundant levels of kNBC1 protein in oocytes injected with wild-type kNBC1 or mutants P**LF**S and **FL**PS on Western blots (Fig. 6). Therefore the kNBC1 mutants P**LF**S and **FL**PS are localized to a membrane fraction in oocytes, consistent with the observation that their functional

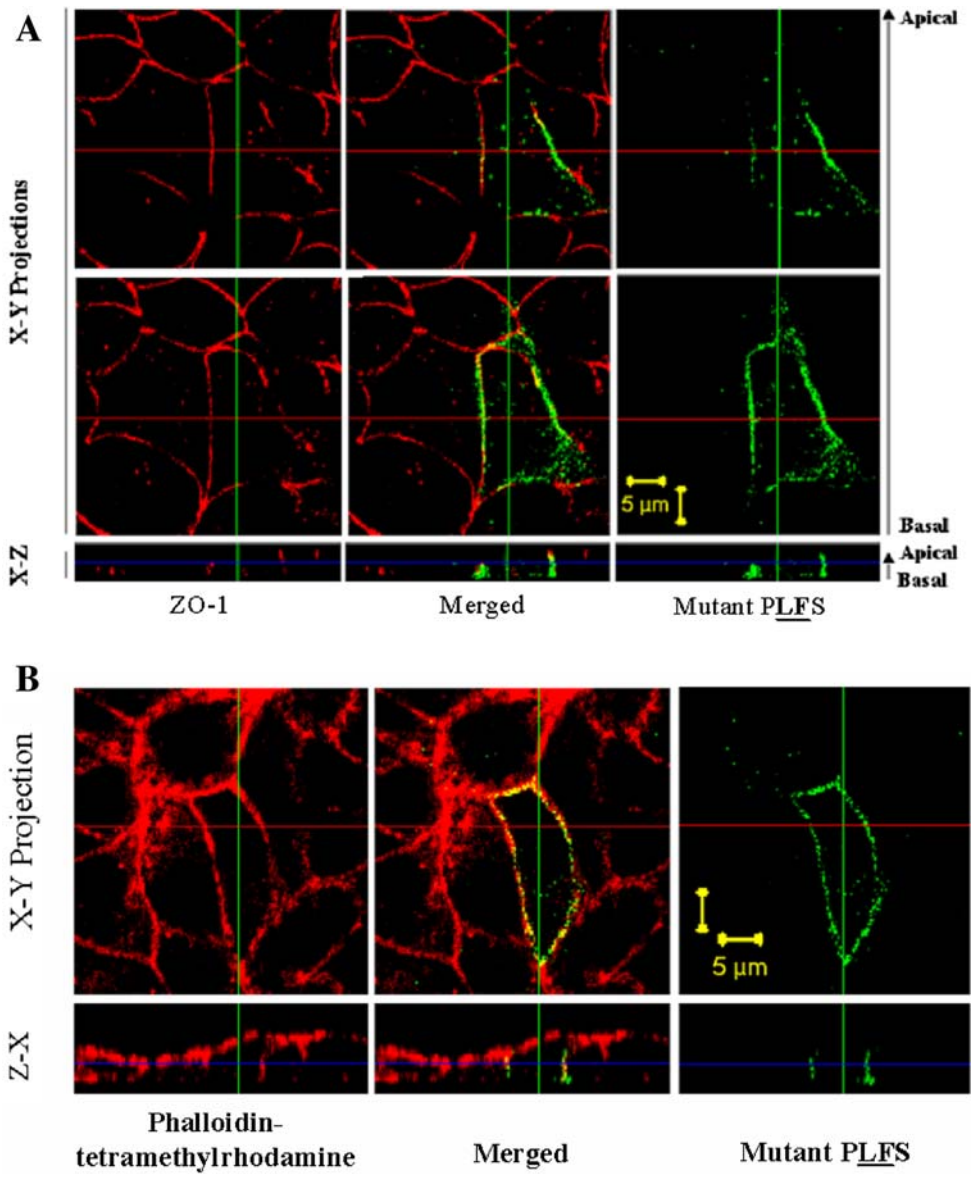

Fig. 2 Transfection of MDCK cells with epitope-tagged NBC1 mutant P**LF**S. **a** Expression of epitope-tagged NBC1 mutant P**LF**S (1010 QQP**LF**S 1015) costained with ZO-1. Z-stack (x-y projections, front view) image analysis (top and middle). As demonstrated, NBC1 mutant P**LF**S, with a reversed dihydrophobic FL motif, is targeted at the plasma membrane. Z-line(x-z projection, side view) image analysis(bottom panel). The NBC1 mutant P**LF**S is targeted at the basolateral membrane. **b** Expression of epitope-tagged NBC1 mutant P**LF**S (1010 QQP**LF**S 1015) costained with phalloidin-tetramethylrhodamine. Z-stack (x-y projection, front view) image analysis (top). As demonstrated, NBC1 mutant P**LF**S, with a reversed dihydrophobic FL motif, is targeted at the plasma membrane. Z-line (z-x projection, side view) image analysis (bottom). NBC1 mutant P**LF**S is targeted at the basolateral membrane. Green, GFP-NBC1; red, phalloidin-tetramethylrhodamine staining

activities do not differ from those of wild-type kNBC1 (Figs. 2 and 3).

The kNBC1 mutant PS**FL** was also abundantly expressed in oocytes and localized to a membrane fraction (Fig. 6); however, since its functional activity was reduced compared with the wild type, we examined its subcellular localization by immunocytochemistry. The PS**FL**-containing NBC1 mutant was injected into oocytes and immunostained with anti GFP-antibodies or transfected into MDCK cells and costained with PDI antibody, an ER marker. As shown in Fig. 7a, oocyte plasma membrane expression of the NBC1 mutant PS**FL** was significantly reduced relative to the wild-type NBC1 cRNA. In transfected MDCK cells, the epitope-tagged kNBC1 PS**FL** mutant colocalized with the ER marker PDI (Fig. 7b), suggesting that the reduced activity of PSFL results from its failure to translocate efficiently to the plasma membrane.

The Basolateral-Targeted Dihydrophobic FL Motif Shows an α-Helical Structure: Effect on α-Helical Content of Reversing or Shifting the Motif Downstream

To investigate the effects of FL motif mutation on the secondary structure of the C-terminal cytoplasmic tail, three 20-amino-acid peptides were synthesized. These peptides corresponded to wild-type $kNBC1_{I1001\text{-}S1020}$ (IKIPMDIMEQQP**FL**SDSKPS), kNBC1 mutant P**LF**S (IKIPMDIMEQQP**LF**SDSKPS), and kNBC1 mutant PS**FL** (IKIPMDIMEQQPS**FL**DSKPS). Peptides were synthesized with purities >95%.

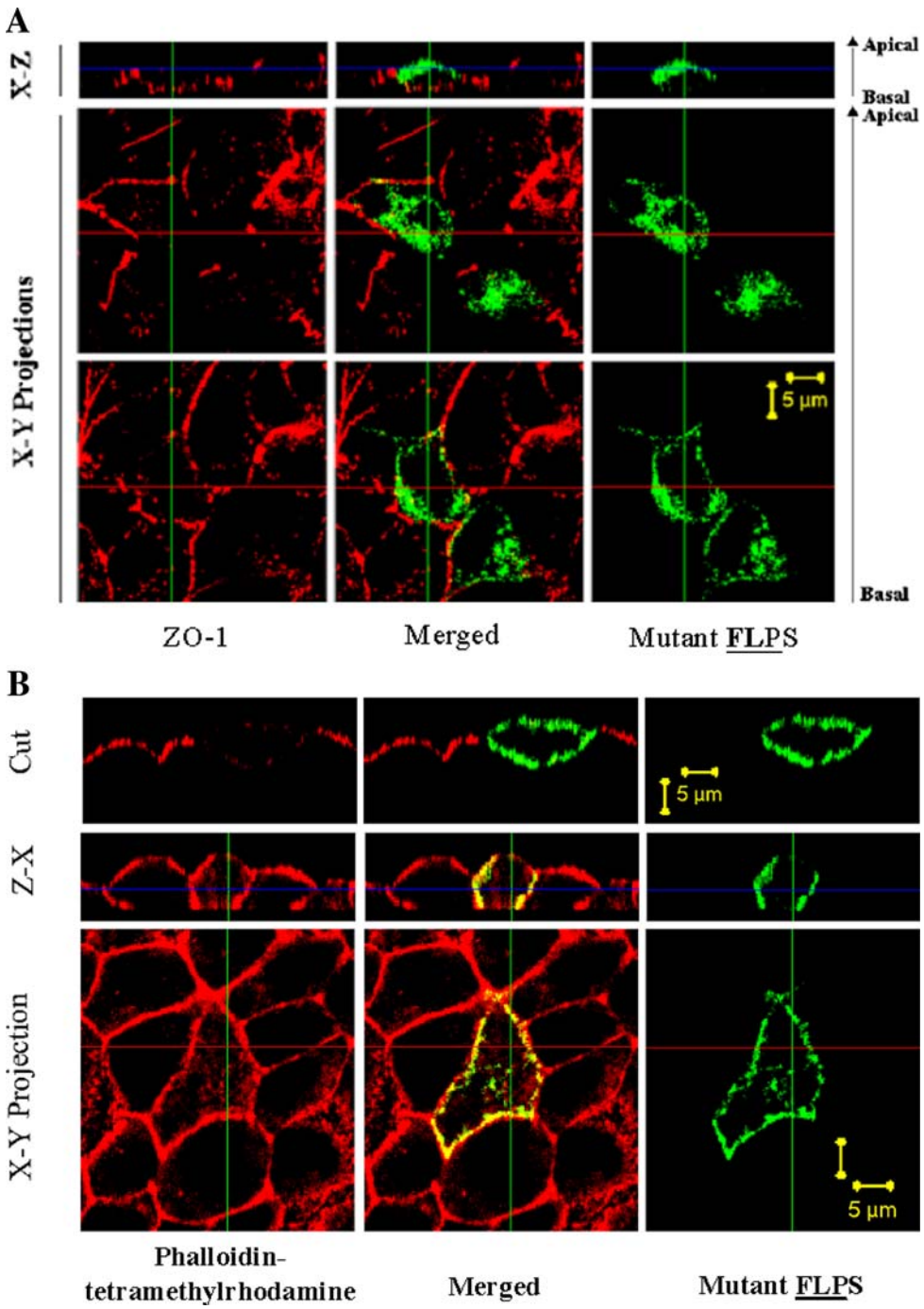

Fig. 3 Transfection of MDCK cells with epitope-tagged NBC1 mutant **FL**PS. **a** Expression of the epitope-tagged NBC1 mutant **FL**PS (1010 QQ**FL**PS 1015) costained with ZO-1. Z-stack (x-y projections, front view) image analysis (bottom and middle). As demonstrated, NBC1 mutant **FL**PS, with a dihydrophobic FL motif shifted upstream, is targeted at the plasma membrane. Z-line (x-z projection, side view) image analysis (top). The NBC1 mutant **FL**PS is mistargeted at the apical membrane. **b** Expression of the epitope-tagged NBC1 mutant **FL**PS (1010 QQ**FL**PS 1015) costained with phalloidin-tetramethylrhodamine and PNA-lectin. Z-stack (x-y projection, front view) image analysis (bottom). As demonstrated, NBC1 mutant **FL**PS, with the dihydrophobic FL motif shifted upstream, is targeted at the plasma membrane. Z-line (x-z projection, side view) image analysis (middle). The NBC1 mutant **FL**PS is mistargeted at the apical membrane. Green, GFP-NBC1; red, phalloidin-tetramethylrhodamine staining. Cut image (side view) analysis (top) showed that the NBC1 mutant **FL**PS is mistargeted at the apical membrane. Green, GFP-NBC1; red, PNA-lectin staining with Alexa-Fluor 568

Secondary structures of these peptides were evaluated with CD (Fig. 8). In phosphate buffer, the wild-type peptide adopted a secondary structure with significant helical character, as evidenced by its two minima, one at 208–210 nm and the other at 222 nm (Fig. 8a). These double minima are characteristic of a helical structure (Greenfield 2006). In stark contrast, this helical character was abolished for both mutant peptides. Rather than exhibiting the double minimum shown by the wild-type peptide, both mutants exhibited a single strong minimum near 200 nm, indicating that these peptides adopted a disordered, extended structure (Greenfield 2006). Moreover, the spectra of the two mutant peptides were nearly identical, indicating that either mutation was sufficient to abolish the helicity of the C-terminal cytoplasmic tail. In 50% TFE, which tends to favor α-helix formation, the three peptides behaved similarly, with the wild-type peptide exhibiting a double minimum at 208 and 224 nm, indicative of a significant helical character, and the mutant peptides both exhibiting a strong minimum at

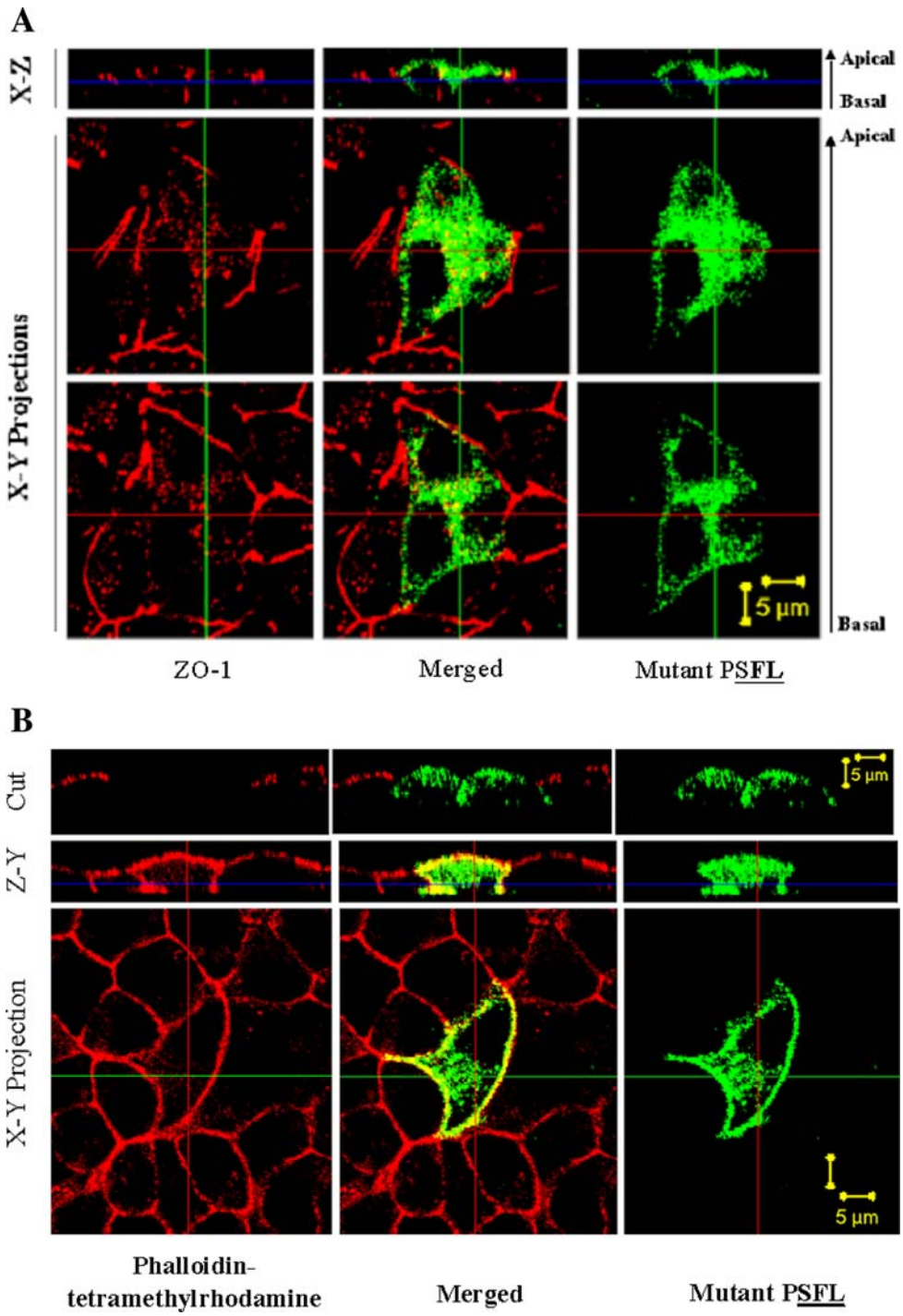

Fig. 4 Transfection of MDCK cells with epitope-tagged NBC1 mutant PS**FL**. **a** Expression of the epitope-tagged NBC1 mutant PS**FL** (1010 QQPS**FL** 1015) costained with ZO-1. Z-stack (x-y projections, front view) image analysis (bottom and middle). As demonstrated, NBC1 mutant PS**FL**, with the dihydrophobic FL motif shifted downstream, is mistargeted at the cytoplasm. Z-line (x-z projection, side view) image analysis (top). The NBC1 mutant PS**FL** is mistargeted at the apical membrane. Green, GFP-NBC1 mutants; red, ZO-1 staining with Alexa-Fluor 568. **b** Expression of the epitope-tagged NBC1 mutant PS**FL** (1010 QQPS**FL** 1015) costained with phalloidin-tetramethyl-rhodamine and PNA-lectin. Z-stack (x-y projection, front view) image analysis (bottom). As indicated, NBC1 mutant PS**FL**, with the dihydrophobic FL motif shifted downstream, is mistargeted at the cytoplasm. Z-line (z-y projection, side view) image analysis (middle). The NBC1 mutant PS**FL** is mistargeted at the apical membrane. Green, GFP-NBC1 mutants; red, phalloidin-tetramethylrhodamine staining. Cut image (side view) analysis (top) showed that the NBC1 mutant PS**FL** is mistargeted at the apical membrane. Green, GFP-NBC1 mutants; red, PNA-lectin staining with Alexa-Fluor 568

202–204 nm (Fig. 8b). These data show that reversing the dihydrophobic **FL** motif (mutant P**LF**S) or shifting it downstream (mutant PS**FL**) caused a significant reduction in the helicity of the C-terminal cytoplasmic tail, both in water and in 50% TFE. Further investigations on the tertiary structure of kNBC1 by more precise methods such as x-ray diffraction or two-dimensional NMR would help to further elucidate the structure of the cytoplasmic tail for the full protein.

Discussion

The specific orientation and flexibility of the primary sequence of the dihydrophobic FL motif in the C-terminal fragment of kNBC1 were tested as determinants of basolateral membrane targeting, functional activity, and secondary structure. The results demonstrated that reversing the FL motif from P**FL**S to P**LF**S did not affect the basolateral membrane targeting or functional activity of

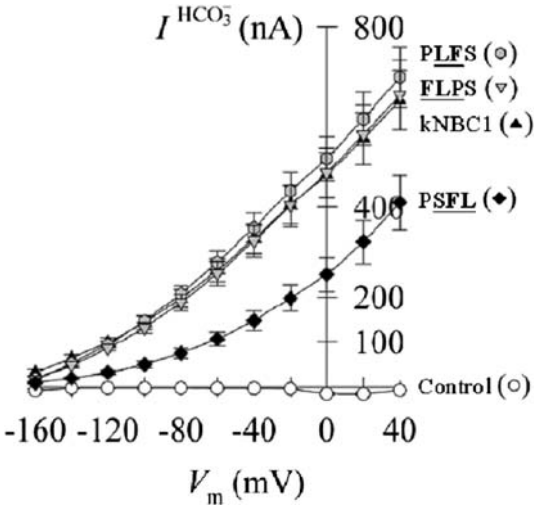

Fig. 5 Effect of FL motif mutations on the functional activity of kNBC1 expressed in oocytes. We measured currents evoked by the addition of 33 mM HCO_3^- (5.6% CO_2) in control oocytes (open circles; $n = 16$) and oocytes expressing wild-type kNBC1 (black triangles; $n = 16$) or the kNBC1 mutants P**LF**S (gray hexagons; $n = 9$), **FL**PS (gray inverted triangles; $n = 16$), and P**SFL** (black diamonds; $n = 16$). Currents for wild-type kNBC1 and mutants P**LF**S and **FL**PS did not differ at any V_m ($p > 0.13$). Currents for the kNBC1 mutant P**SFL** differed from those of all other groups between −60 and +40 mV ($p < 0.01$)

NBC1 (Figs. 2 and 5). These results strongly indicate that specific orientation of the dihydrophobic motif FL is not a constraint for NBC1 to target the basolateral membrane in polarized MDCK cells.

Our previous studies demonstrated that mutagenizing FL to FF (dihydrophobic motif FL > FF) does not affect basolateral membrane targeting, whereas mutagenizing it to LL (dihydrophobic motif FL > LL) causes mistargeting at the cytoplasm in polarized MDCK cells (Li et al. 2007). Taken together, these results indicate that F(phenylalanine) can substitute for L (leucine) without affecting the basolateral membrane targeting of kNBC1, whereas, substituting F with L alters the exclusivity of basolateral membrane targeting of the cotransporter. These results indicate that the precise position of F (phenylalanine) residue in the dihydrophobic motif (FL or LF) is not an impediment to the basolateral targeting of NBC1. Western blotting in oocyte membranes showed that kNCB1 mutants that are functionally active are detected in the detergent fraction, which is consistent with their plasma membrane localization in MDCK cells.

The relative positions (flexibility of primary sequence) of the dihydrophobic FL motif in the C-terminal domain were demonstrated to be constraints to basolateral targeting, as well as the functionality of NBC1. First, an upstream shift of the FL motif by one amino acid residue (P**FL**S to **FL**PS) caused the mistargeting of sodium bicarbonate cotransporter to the apical membrane (Fig. 3a, b). Like other apically mistargeted mutants {FL > AL (F1013A) and FL > FA (L1014A)} (Li et al. 2004), the functional activity of the mutant **FL**PS was comparable to that of the wild-type NBC1 (Fig. 5). Western blotting on oocyte membranes showed that the kNCB1 **FL**PS mutant was detected in the detergent (membrane)-containing fraction (Fig. 6).

Interestingly, shifting the FL motif downstream by one amino acid residue (P**FL**S to PS**FL**) caused accumulation of NBC1 in the cytoplasm in polarized MDCK cells (Fig. 4a, b), along with a significant reduction in its functional activity in oocytes, as shown in Fig. 5. Immunostaining and Western blotting showed that the surface expression of kNCB1 mutant PS**FL** in oocytes' plasma membrane is noticeably reduced in comparison with the kNBC1 wild-type. GFP-kNBC1 mutant PS**FL** colocalized with the ER marker PDI when merged images were acquired in transiently transfected MDCK cells (Fig. 7b). These results indicate that downward shifting of the FL motif by even one amino acid residue interferes with the

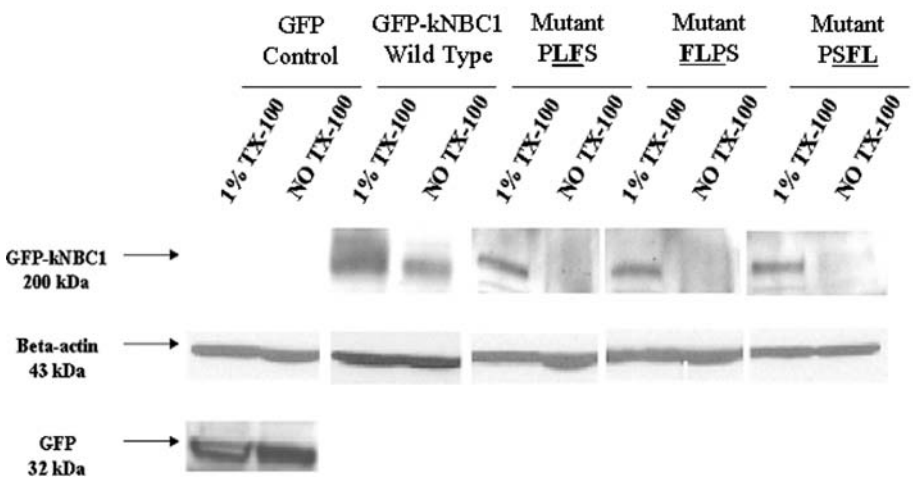

Fig. 6 Western blot analysis of the epitope-tagged kNBC1 and its mutants in frog oocytes. Oocytes injected with GFP, full-length GFP-kNBC1, and its mutants' cRNAs were homogenized in lysis buffer with or without 1% Triton X-100. Rabbit anti-GFP serum was used to detect the GFP signal either from GFP only or from GFP-fused kNBC1 proteins. The same blot membranes were normalized with β-actin expression

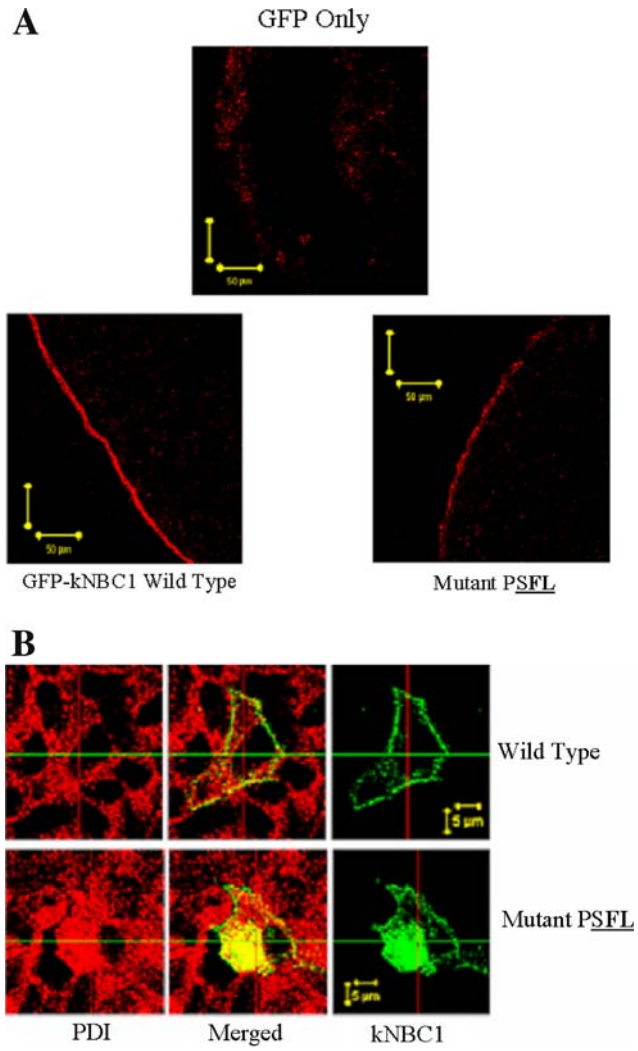

Fig. 7 Subcellular localization of the NBC1 P**SFL** mutant expressed in *Xenopus* oocytes and MDCK cells. **a** Expression of epitope-tagged wild-type kNBC1 and mutant P**SFL** in oocytes. Scale bar, 50 μm. **b** Immunostaining of MDCK cells expressing epitope-tagged kNBC1 wild-type and P**SFL** mutant with an ER marker antibody, PDI

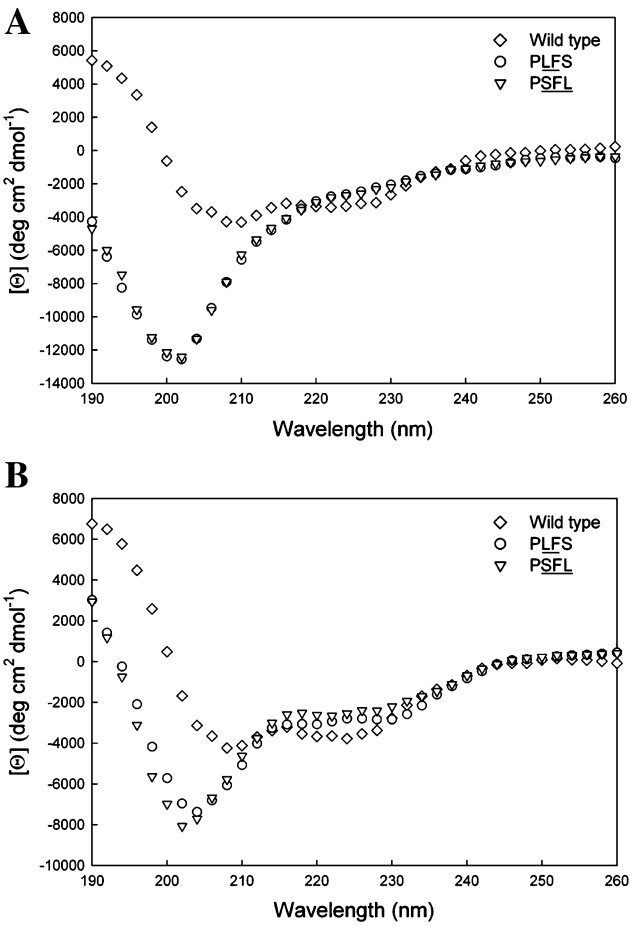

Fig. 8 Circular dichroism of wild-type $kNBC1_{I1001\text{-}S1020}$ peptide (◇), peptide P**LFS**, corresponding to kNBC mutant P**LFS** (○), and peptide P**SFL**, corresponding to kNBC mutant P**SFL** (▽). Spectra collected at a 60 μM peptide concentration in 10 mM sodium phosphate, 10 mM potassium fluoride (**a**) and in the same buffer with 50% (**b**)

plasma membrane localization of NBC1 in epithelial cells. Along with its retention in the cytoplasm, the activity of the P**SFL**-containing mutant was significantly decreased (Fig. 5).

Our data therefore reveal that the relative position of the dihydrophobic FL motif in kNBC1 protein is very rigid. The nonflexibility of the dihydrophobic FL motif position may be sustained conformationally by the whole kNBC1 protein structure or short peptide scaffolds. Although there are many reports on the mechanisms of basolateral membrane targeting of membrane proteins, most studies have focused on the identification of primary amino acid residues or related adaptor-protein complexes, with few attempting to characterize the tertiary or secondary structure of such basolateral targeting motifs. In addition to examining the impact of the specific orientation and relative position of the dihydrophobic FL motif on the basolateral targeting and functional activity of NBC1, we investigated how the orientation and relative positioning of the dihydrophobic FL motif affected secondary structures of kNBC1 peptides. The peptides are designed to have proper lengths to contain the FL motif or shifted FL motif near the middle of whole sequences in order to detect any typical secondary structures or their changes, having well-charged amino acid residues being soluble in water or relevant buffers. Further, we explored how this motif's secondary structure changed when these mutations were made. We found that peptides corresponding to the dihydrophobic FL motif contained a significant α-helical structure, whereas peptides with a reversed FL motif or a C-terminal-shifted FL motif were disordered (Fig. 8). There was no direct correlation between disordered secondary structures of the FL dihydrophobic motif and

Table 1 Summary of the impact of various FL mutations on NBC1

kNBC1	Targeting	Secondary structure	Function
Wild-type P**FL**S	Basolateral	α-Helical	****
Mutant P**LF**S, reversed FL motif	Basolateral	Disordered	****
Mutant **FL**PS, N-terminal FL shift	Apical & cytoplasm		****
Mutant PS**FL**, C-terminal FL shift	Cytoplasm & apical	Disordered	**

exclusive basolateral targeting of the NBC1 protein. Table 1 summarizes the effect of various mutations involving the C-terminal FL motif on the function, membrane targeting, and α-helical structure of NBC1.

We conclude that the relative position of amino acid residues FL motif in the C-terminal cytoplasmic domain is essential for the efficient basolateral localization of NBC1. We further conclude that the primary sequence of the dihydrophobic FL motif in the C-terminal end plays an important role in the α-helical structure of NBC1.

Acknowledgments These studies were supported by National Institute of Health Grant DK 62809 (to M.S.) and a Merit Review Award and grants from Dialysis Clinic Incorporated (to M.S).

References

Abuladze N, Azimov R, Newman D, Sassani P, Liu W, Tatishchev S, Pushkin A, Kurtz I (2005) Critical amino acid residues involved in the electrogenic sodium-bicarbonate cotransporter kNBC1-mediated transport. J Physiol 565:717–730

Alper SL (2002) Genetic diseases of acid-base transporters. Annu Rev Physiol 64:899–923

Bai X, Chen X, Feng Z, Hou K, Zhang P, Fu B, Shi S (2006) Identification of basolateral membrane targeting signal of human sodium-dependent dicarboxylate transporter 3. J Cell Physiol 206:821–830

Barman S, Ali A, Hui EK, Adhikary L, Nayak DP (2001) Transport of viral proteins to the apical membranes and interaction of matrix protein with glycoproteins in the assembly of influenza viruses. Virus Res 77:61–69

Bello V, Goding JW, Greengrass V, Sali A, Dubljevic V, Lenoir C, Trugnan G, Maurice M (2001) Characterization of a di-leucine-based signal in the cytoplasmic tail of the nucleotide-pyrophosphatase NPP1 that mediates basolateral targeting but not enocytosis. Mol Biol Cell 12:3004–3015

Bok D, Schibler MJ, Pushkin A, Sassani P, Abuladze N, Naser Z, Kurtz I (2001) Immunolocalization of electrogenic sodium-bicarbonate cotransporters pNBC1 and kNBC1 in the rat eye. Am J Physiol Renal Physiol 281:F920–F935

Boron WF (2006) Acid-base transport by the renal proximal tubule. J Am Soc Nephrol 17:2368–2382

Brown DA, Rose JK (1992) Sorting GPI-anchored proteins to glycolipid-enriched membrane subdomains during transport to the apical cell surface. Cell 68:533–544

Burnham CE, Amlal H, Wang Z, Shull GE, Soleimani M (1997) Cloning and functional expression of a human kidney Na^+:HCO_3^- cotransporter. J Biol Chem 272:19111–19114

Devonald MA, Smith AN, Poon JP, Ihrke G, Karet FE (2003) Non-polarized targeting of AE1 causes autosomal dominant distal renal tubular acidosis. Nat Genet 33:125–127

Dinour D, Chang MH, Satoh J, Smith BL, Angle N, Knecht A, Serban I, Holtzman EJ, Romero MF (2004) A novel missense mutation in the sodium bicarbonate cotransporter (NBCe1/SLC4A4) causes proximal tubular acidosis and glaucoma through ion transport defects. J Biol Chem 279:52238–52246

Grati M, Aggarwal N, Strehler EE, Wenthold RJ (2006) Molecular determinants for differential membrane trafficking of PMCA1 and PMCA2 in mammalian hair cells. J Cell Sci 119:2995–3007

Greenfield NJ (2006) Using circular dichroism spectra to estimate protein secondary structure. Nat Protoc 1:2876–2890

Gut A, Kappeler F, Hyka N, Balda MS, Hauri HP, Matter K (1998) Carbohydrate-mediated Golgi to cell surface transport and apical targeting of membrane proteins. EMBO J 17:1919–1929

Horita S, Yamada H, Inatomi J, Moriyama N, Sekine T, Igarashi T, Endo Y, Dasouki M, Ekim M, Al-Gazali L, Shimadzu M, Seki G, Fujita T (2005) Functional analysis of NBC1 mutants associated with proximal renal tubular acidosis and ocular abnormalities. J Am Soc Nephrol 16:2270–2278

Hunziker W, Fumey C (1994) A di-leucine motif mediates endocytosis and basolateral sorting of macrophage IgG Fc receptors in MDCK cells. EMBO J 13:2963–2969

Igarashi T, Inatomi J, Sekine T, Cha SH, Kanai Y, Kunimi M, Tsukamoto K, Satoh H, Shimadzu M, Tozawa F, Mori T, Shiobara M, Seki G, Endou H (1999) Mutations in SLC4A4 cause permanent isolated proximal renal tubular acidosis with ocular abnormalities. Nat Genet 23:264–266

Igarashi T, Inatomi J, Sekine T, Seki G, Shimadzu M, Tozawa F, Takeshima Y, Takumi T, Takahashi T, Yoshikawa N, Nakamura H, Endou H (2001) Novel nonsense mutation in the Na^+/HCO_3^- cotransporter gene (SLC4A4) in a patient with permanent isolated proximal renal tubular acidosis and bilateral glaucoma. J Am Soc Nephrol 12:713–718

Ikonen E (2001) Roles of lipid rafts in membrane transport. Curr Opin Cell Biol 13:470–477

Kundu A, Avalos RT, Sanderson CM, Nayak DP (1996) Transmembrane domain of influenza virus neuraminidase, a type II protein, possesses an apical sorting signal in polarized MDCK cells. J Virol 70:6508–6515

Li HC, Worrell RT, Matthews JB, Husseinzadeh H, Neumeier L, Petrovic S, Conforti L, Soleimani M (2004) Identification of a carboxyl-terminal motif essential for the targeting of Na^+–HCO_3^- cotransporter NBC1 to the basolateral membrane. J Biol Chem 279:43190–43197

Li HC, Szigligeti P, Worrell RT, Matthews JB, Conforti L, Soleimani M (2005) Missense mutations in Na^+:HCO_3^- cotransporter NBC1 show abnormal trafficking in polarized kidney cells: a basis of proximal renal tubular acidosis. Am J Physiol Renal Physiol 289:F61–F71

Li HC, Li EY, Neumeier L, Conforti L, Soleimani M (2007) Identification of a novel signal in the cytoplasmic tail of the Na^+:HCO_3^- cotransporter NBC1 that mediates basolateral targeting. Am J Physiol Renal Physiol 292:F1245–F1255

Lin S, Naim HY, Rodriguez AC, Roth MG (1998) Mutations in the middle of the transmembrane domain reverse the polarity of

transport of the influenza virus hemagglutinin in MDCK epithelial cells. J Cell Biol 142:51–57

Mackenzie B (1999) Selected techniques in membrane transport. In: Biomembrane transport. Academic Press, San Diego, pp 327–342

Mackenzie B, Takanaga H, Hubert N, Rolfs A, Hediger MA (2007) Functional properties of multiple isoforms of human divalent metal-ion transporter 1 (DMT1). Biochem J 403:59–69

Matter K, Hunziker W, Mellman I (1992) Basolateral sorting of LDL receptor in MDCK cells: the cytoplasmic domain contains two tyrosine-dependent targeting determinants. Cell 71:741–753

Matter K, Mellman I (1994) Mechanisms of cell polarity: sorting and transport in epithelial cells. Curr Opin Cell Biol 6:545–554

Matter K, Yamamoto EM, Mellman I (1994) Structural requirements and sequence motifs for polarized sorting and endocytosis of LDL and Fc receptors in MDCK cells. J Cell Biol 126:991–1004

Miranda KC, Khromykh T, Christy P, Le TL, Gottardi CJ, Yap AS, Stow JL, Teasdale RD (2001) A dileucine motif targets E-cadherin to the basolateral cell surface in Madin-Darby canine kidney and LLC-PK1 epithelial cells. J Biol Chem 276:22565–22572

Muth TR, Caplan MJ (2003) Transport protein trafficking in polarized cells. Annu Rev Cell Dev Biol 19:333–366

Pena-Munzenmayer G, Catalan M, Cornejo I, Figueroa CD, Melvin JE, Niemeyer MI, Cid LP, Sepulveda FV (2005) Basolateral localization of native ClC-2 chloride channels in absorptive intestinal epithelial cells and basolateral sorting encoded by a CBS-2 domain di-leucine motif. J Cell Sci 118:4243–4252

Pushkin A, Kurtz I (2006) SLC4 base(HCO_3^-, CO_3^{2-}) transporters: classification, function, structure, genetic diseases, and knockout models. Am J Physiol Renal Physiol 290:F580–F599

Regeer RR, Markovich D (2004) A dileucine motif targets the sulfate anion transporter sat-1 to the basolateral membrane in renal cell lines. Am J Physiol Cell Physiol 287:C365–C372

Romero MF (2005) Molecular pathophysiology of SLC4 bicarbonate transporters. Curr Opin Nephrol Hypertens 14:495–501

Romero MF, Hediger MA, Boulpaep EL, Boron WF (1997) Expression cloning and characterization of a renal electrogenic Na^+/HCO_3^- cotransporter. Nature 387:409–413

Romero MF, Fulton CM, Boron WF (2004) The SLC4 family of HCO_3–transporters. Pflugers Arch 447:495–509

Roussa E, Romero MF, Schmitt BM, Boron WF, Alper SL, Thevenod F (1999) Immunolocalization of anion exchanger AE2 and Na(+)–HCO(–)(3) cotransporter in rat parotid and submandibular glands. Am J Physiol 277:G1288–G1296

Scheiffele P, Peranen J, Simons K (1995) N-Glycans as apical sorting signals in epithelial cells. Nature 378:96–98

Schmitt BM, Biemesderfer D, Romero MF, Boulpaep EL, Boron WF (1999) Immunolocalization of the electrogenic Na^+–HCO_3^- cotransporter in mammalian and amphibian kidney. Am J Physiol Renal Physiol 276:F27–F38

Sheikh H, Isacke CM (1996) A di-hydrophobic Leu-Val motif regulates the basolateral localization of CD44 in polarized Madin-Darby canine kidney epithelial cells. J Biol Chem 271:12185–12190

Simons K, Ikonen E (1997) Functional rafts in cell membrane. Nature 387:569–572

Soleimani M (2002) Na^+:HCO_3^- cotransporters (NBC): expression and regulation in the kidney. J Nephrol 15(Suppl 5):S32–S40

Soleimani M (2003) Functional and molecular properties of Na^+:HCO_3^- cotransporters (NBC). Minerva Urol Nefrol 55:131–140

Soleimani M, Burnham CE (2001) Na^+:HCO_3^- cotransporters (NBC): cloning and characterization. J Membr Biol 183:71–84

Tanemoto M, Abe T, Ito S (2005) PDZ-binding and di-hydrophobic motifs regulate distribution of Kir4.1 channels in renal cells. J Am Soc Nephrol 16:2608–2614

Tepass U, Tanentzapf G, Ward R, Fehon R (2001) Epithelial cell polarity and cell junctions in *Drosophila*. Annu Rev Genet 35:747–784

Thevenod F, Roussa E, Schmitt BM, Romero MF (1999) Cloning and immunolocalization of a rat pancreatic Na(+) bicarbonate cotransporter. Biochem Biophys Res Commun 264:291–298

Thomas DC, Brewer CB, Roth MG (1993) Vesicular stomatitis virus glycoprotein contains a dominant cytoplasmic basolateral sorting signal critically dependent upon a tyrosine. J Biol Chem 268:3313–3320

Toye AM, Parker MD, Daly CM, Lu J, Virkki LV, Pelletier MF, Boron WF (2006) The human NBCe1-A mutant R881C, associated with proximal renal tubular acidosis, retains function but is mistargeted in polarized renal epithelia. Am J Physiol Cell Physiol 291:C788–C801

Usui T, Hara M, Satoh H, Moriyama N, Kagaya H, Amano S, Oshika T, Ishii Y, Ibaraki N, Hara C, Kunimi M, Noiri E, Tsukamoto K, Inatomi J, Kawakami H, Endou H, Igarashi T, Goto A, Fujita T, Araie M, Seki G (2001) Molecular basis of ocular abnormalities associated with proximal renal tubular acidosis. J Clin Invest 108:107–115

Xu J, Wang ZH, Barone S, Petrovic M, Amlal H, Conforti L, Petrovic S, Soleimani M (2003) Expression of the Na^+–HCO_3^- cotransporter NBC4 in rat kidney and characterization of a novel NBC4 variant. Am J Physiol Renal Physiol 284:F41–F50

Yamada H, Yamazaki S, Moriyama N, Hara C, Horita S, Enomoto Y, Kudo A, Kawakami H, Tanaka Y, Fujita T, Seki G (2003) Localization of NBC-1 variants in human kidney and renal cell carcinoma. Biochem Biophys Res Commun 310:1213–1218

Zou Z, Chung B, Nguyen T, Mentone S, Thomson B, Biemesderfer D (2004) Linking receptor-mediated endocytosis and cell signaling: evidence for regulated intramembrane proteolysis of megalin in proximal tubule. J Biol Chem 279:34302–34310